

# Privileged Phosphine-Based Metal–Organic Frameworks for Broad-Scope Asymmetric Catalysis

Joseph M. Falkowski,<sup>‡,†</sup> Takahiro Sawano,<sup>‡,†</sup> Teng Zhang,<sup>‡</sup> Galen Tsun,<sup>§</sup> Yuan Chen,<sup>‡</sup> Jenny V. Lockard,<sup>‡</sup> and Wenbin Lin<sup>\*,‡</sup>

<sup>‡</sup>Department of Chemistry, University of Chicago, 929 East 57th Street, Chicago, Illinois 60637, United States

<sup>§</sup>Department of Chemistry, CB#3290, University of North Carolina, Chapel Hill, North Carolina 27599, United States

<sup>‡</sup>Department of Chemistry, Rutgers University, 73 Warren Street, Newark, New Jersey 07102, United States

**S** Supporting Information

**ABSTRACT:** A robust and porous Zr metal–organic framework (MOF) based on a BINAP-derived dicarboxylate linker, BINAP-MOF, was synthesized and post-synthetically metalated with Ru and Rh complexes to afford highly enantioselective catalysts for important organic transformations. The Rh-functionalized MOF is not only highly enantioselective (up to >99% ee) but also 3 times as active as the homogeneous control. XAFS studies revealed that the Ru-functionalized MOF contains Ru-BINAP precatalysts with the same coordination environment as the homogeneous Ru complex. The post-synthetically metalated BINAP-MOFs provide a versatile family of single-site solid catalysts for catalyzing a broad scope of asymmetric organic transformations, including addition of aryl and alkyl groups to  $\alpha,\beta$ -unsaturated ketones and hydrogenation of substituted alkene and carbonyl compounds.

As an emerging class of porous molecular materials,<sup>1</sup> metal–organic frameworks (MOFs) provide a highly tunable platform to engineer heterogeneous catalysts for important reactions, e.g., asymmetric organic transformations, that cannot be achieved with traditional porous inorganic materials.<sup>2</sup> Among the asymmetric MOF catalysts reported to date, the most efficient examples all contain a privileged chiral ligand as the means for enantio-differentiation.<sup>3</sup> The first MOF catalyst with significant enantiomeric excesses (ee's) contained the  $C_2$ -symmetric 1,1'-bi-2-naphthol (BINOL).<sup>4</sup> The post-synthetically generated Ti-BINOLate moiety in the chiral MOF was responsible for high ee's observed for diethylzinc additions to aromatic aldehydes.<sup>4b</sup> Subsequently, a Mn-salen-based MOF was used for asymmetric epoxidation of alkenes.<sup>5</sup> Since these reports, multiple stereoselective MOF catalysts have been developed based on BINOL- and salen-based ligands.<sup>6</sup>

Of the pantheon of privileged chiral ligands, 2,2'-bis(diphenylphosphino)-1,1'-binaphthyl (BINAP) has received the most attention in the homogeneous catalysis community.<sup>7</sup> Since the design of this  $C_2$ -symmetric ligand by Noyori et al. in 1980, BINAP has been used as a source of chirality in many late transition metal-catalyzed reactions and is the gold standard when developing new chiral bisphosphine ligands.<sup>8</sup> Despite the importance of the BINAP ligand, it has not yet been used in the

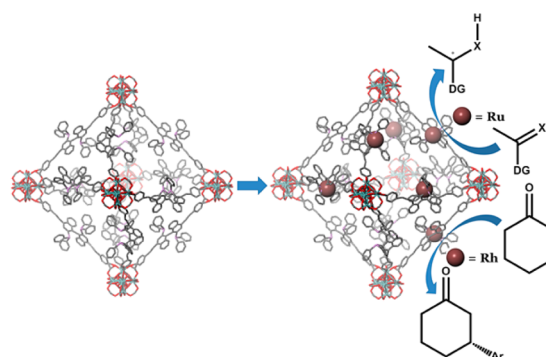


**Figure 1.** Post-synthetic metalation of BINAP-MOF (1) and representative catalytic activities of metalated MOFs.

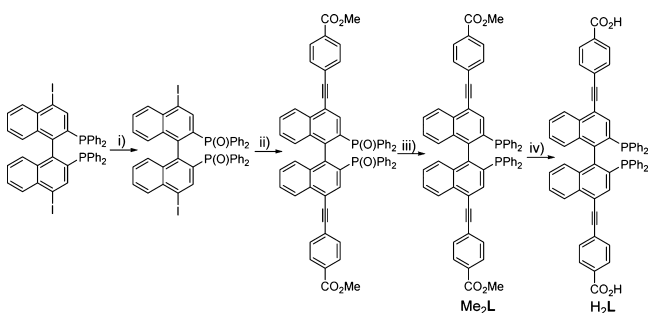
construction of MOF-based asymmetric catalysts, attributed to the difficulty in synthesizing bridging ligands based on chiral bisphosphines and the sensitivity of phosphines to the conditions used in typical MOF crystal growth. Lin et al. reported an amorphous Zr-phosphonate system containing Ru-BINAP precatalysts for hydrogenation of both  $\beta$ -keto esters and aromatic ketones.<sup>9</sup> However, only a small fraction of the catalysts on the surfaces of these Zr-phosphonate particles is active in asymmetric hydrogenation reactions.

We report here the first chiral MOF based on a BINAP-derived dicarboxylate linker (L) and its post-synthetic metalation to afford highly enantioselective catalysts for hydrogenation and aryl/alkyl addition reactions (Figure 1). This BINAP-MOF contains the  $Zr_6O_4(OH)_4(O_2CR)_{12}$  cluster secondary building unit (SBU) and adopts the same framework topology as UiO-66 reported by Lillerud et al.<sup>10</sup> The UiO structure provides an ideal platform to design MOF-based heterogeneous catalysts due to their stability under a range of reaction conditions. We demonstrate that BINAP-MOF is a versatile precursor to multiple catalytic systems through the judicious choice of post-synthetic metalation conditions. The metalated MOF materials are efficient catalysts for asymmetric hydrogenation of substituted alkene and carbonyl compounds and addition of arylboronic acids and  $AlMe_3$  to  $\alpha,\beta$ -unsaturated ketones.

The BINAP-derived dicarboxylic acid,  $H_2L$ , was prepared from 4,4'-I<sub>2</sub>-BINAP<sup>11</sup> in a multistep sequence as shown in Scheme 1.

Received: January 9, 2014

Published: March 31, 2014

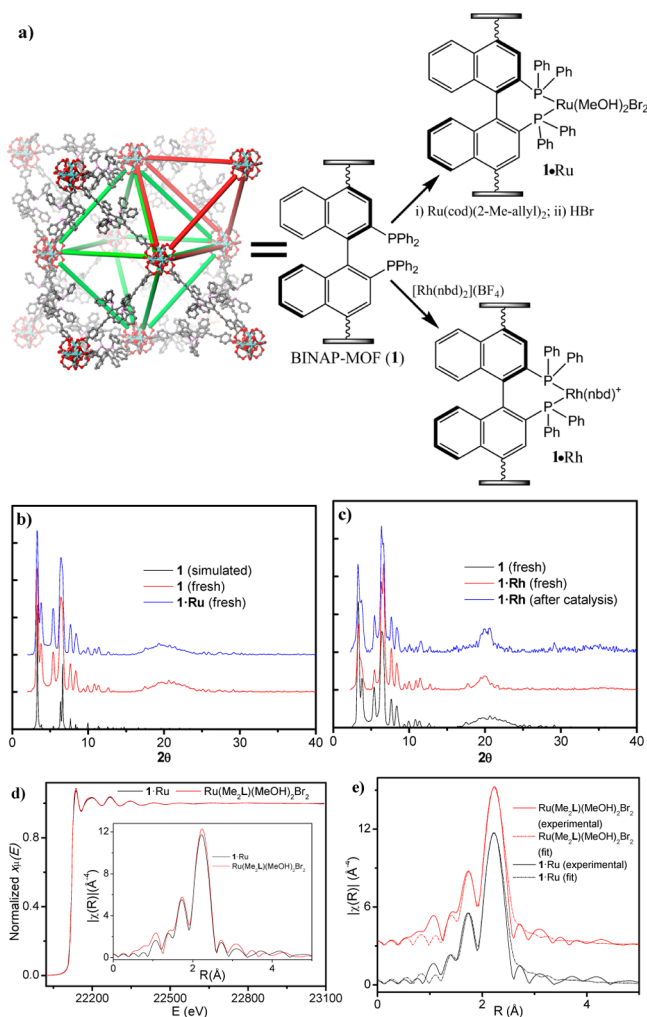
Scheme 1. Synthesis of H<sub>2</sub>L Starting from 4,4'-I<sub>2</sub>-BINAP<sup>a</sup>

<sup>a</sup>Reagents: (i) H<sub>2</sub>O<sub>2</sub>, acetone, 85% yield; (ii) Pd(PPh<sub>3</sub>)<sub>4</sub>, CuI, PPh<sub>3</sub>, methyl 4-ethynylbenzoate, THF/TEA, 67% yield; (iii) HSiCl<sub>3</sub>, TEA, *m*-xylene, 75% yield; (iv) NaOH, THF, EtOH, 95% yield.

4,4'-I<sub>2</sub>-BINAP was oxidized with hydrogen peroxide and coupled with methyl 4-ethynylbenzoate via a Pd-catalyzed Sonogashira reaction to yield 4,4'-bis(methyl-4-carboxyphenylethynyl)-BINAP oxide. Reduction of the BINAP oxide following by saponification led to H<sub>2</sub>L in 41% overall yield.<sup>12</sup> Due to the air-sensitive nature of the phosphine, solvothermal crystal growths of BINAP-MOF were carried out in an air-free environment. A mixture of equimolar H<sub>2</sub>L and ZrCl<sub>4</sub> in dimethylformamide (DMF) and a small amount of trifluoroacetic acid was degassed in a glass tube, flame-sealed under vacuum, and heated at 120 °C for 3 days, to yield the BINAP-MOF (**1**) as colorless octahedral crystals in 44% yield.

**1** crystallizes in the *F*23 chiral space group. The asymmetric unit of **1** contains half of the L ligand and one-twelfth of the Zr<sub>6</sub>O<sub>4</sub>(OH)<sub>4</sub> SBU. The MOF contains both octahedral and tetrahedral cages with edges measuring 23 Å (Figure 2a), but the naphthyl and diphenylphosphino moieties could not be located on the electron density maps due to the free rotation of the C–C single bonds around the ethynyl groups of the L ligand. The solvent-accessible void space was calculated to be 76.3% using PLATON. Thermogravimetric analysis (TGA) of **1** indicated a solvent content of 60% (Figure S1, Supporting Information [SI]), whereas a combination of TGA and NMR solvent analyses gave the complete formula of Zr<sub>6</sub>(OH)<sub>4</sub>O<sub>4</sub>L<sub>6</sub>·126DMF·156H<sub>2</sub>O for **1** (Figure S2). Dye uptake measurements showed that 13.5 wt % of brilliant blue R-250 could be loaded into the channels (Figure S3), indicating the presence of large open channels in **1** that can accommodate large dye molecules and metalating agents. N<sub>2</sub> adsorption measurements did not show porosity for **1**, presumably due to framework distortion upon removal of solvent molecules, which has been observed frequently for mesoporous MOFs with large open channels.<sup>6b,13</sup>

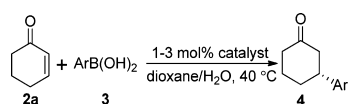
Post-synthetic metalation of **1** was performed by treating with 1 equiv of [Rh(nbd)<sub>2</sub>](BF<sub>4</sub>) to afford **1**·Rh or with 4.9 equiv of Ru(cod)(2-Me-allyl)<sub>2</sub> followed by HBr to afford **1**·Ru (relative to the L equivalents in **1**, SI).<sup>4b,14</sup> Powder X-ray diffraction (PXRD) indicated that the crystallinity of **1** was maintained in both **1**·Rh and **1**·Ru after the metalation reactions. Inductively coupled plasma mass spectrometry (ICP-MS) analyses of the Zr:Rh and Zr:Ru ratios of the digested metalated MOFs gave Rh and Ru loadings of 33% and 50% for **1**·Rh and **1**·Ru, respectively. Although **1**·Rh and **1**·Ru appear to remain single crystalline (SI), the rotational disorder of the L ligands and the partial metalation make it impossible to study the Ru and Rh coordination environments by single-crystal X-ray crystallography. Instead, we resorted to X-ray absorption fine structure spectroscopy (XAFS)



**Figure 2.** (a) Post-synthetic metalation of BINAP-MOF (**1**) to form **1**·Ru and **1**·Rh. (b) PXRD patterns of pristine **1** (simulated from the CIF file, black; experimental, red) and freshly prepared **1**·Ru (blue). (c) PXRD patterns of pristine **1** (black), freshly prepared **1**·Rh (red), and **1**·Rh recovered from AlMe<sub>3</sub> addition reactions (blue). The broad peaks at  $2\theta \approx 20^\circ$  are from the glass capillary tubes. (d) XANES spectra for the Ru K-edge of **1**·Ru (black) and Ru(Me<sub>2</sub>L)(MeOH)<sub>2</sub>Br<sub>2</sub> (red). Inset: Experimental EXAFS spectra in *R* for **1**·Ru (black) and Ru(Me<sub>2</sub>L)(MeOH)<sub>2</sub>Br<sub>2</sub> (red), showing their similarity. (e) Experimental EXAFS spectra in *R* (solid traces) for **1**·Ru and Ru(Me<sub>2</sub>L)(MeOH)<sub>2</sub>Br<sub>2</sub> and fits (dashed lines). The data for Ru(Me<sub>2</sub>L)(MeOH)<sub>2</sub>Br<sub>2</sub> are shifted vertically by 3 units for clarity.

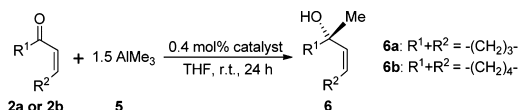
to determine the Ru coordination environment in **1**·Ru.<sup>15</sup> Ru K-edge spectra were collected for powder samples of Ru(Me<sub>2</sub>L)(MeOH)<sub>2</sub>Br<sub>2</sub> and **1**·Ru. Comparison of these data, depicted in Figure 2d,e, reveals nearly identical coordination environments of the Ru ions in the two systems. Further analysis through XAFS data fitting shows that the first coordination shell peak in each case arises from the combination of Ru–P and Ru–O single scattering paths, while the second peak is dominated by the longer Ru–Br scattering path. The scattering path distances and degeneracies derived from these fits are consistent with distorted octahedral coordination of the Ru centers with two P atoms of the L ligand, two methanol solvent molecules, and two Br atoms (Table S2).

A broad scope of catalytic activities was obtained with **1** through the judicious choice of metalating agents. **1**·Rh showed excellent activity in conjugate additions of arylboronic acids to 2-

**Table 1. Asymmetric Additions of Arylboronic Acids to 2-Cyclohexenone by 1·Rh and Homogeneous Catalysts<sup>a</sup>**

entry	Ar	catalyst	cat. loading (mol%)	isolated yield (%)	ee (%) <sup>b</sup>
1	Ph	1·Rh	1	80	>99
2	<i>m</i> -MeCO <sub>2</sub> Ph	1·Rh	1	85	>99
3	<i>p</i> -MeC(O)-Ph	1·Rh	1	99	99
4	Ph	Rh-H <sub>2</sub> L <sup>c</sup>	3	0	N/A
5	Ph	Rh-Me <sub>2</sub> L <sup>c</sup>	3	7 <sup>d</sup>	N/A
6	Ph	Rh-BINAP	1	29	>99
7	<i>m</i> -MeCO <sub>2</sub> Ph	Rh-BINAP	1	34	>99
8	<i>p</i> -MeC(O)-Ph	Rh-BINAP	1	46	>99
9	Ph	Rh-BINAP	3	85	>99
10	<i>m</i> -MeCO <sub>2</sub> Ph	Rh-BINAP	3	87	99
11	<i>p</i> -MeC(O)-Ph	Rh-BINAP	3	87	>99

<sup>a</sup>Reaction conditions: **2a** (1 equiv), **3** (3 equiv), NEt<sub>3</sub> (1 equiv), catalyst (1 or 3 mol% Rh), 1,4-dioxane (0.04 M), H<sub>2</sub>O (0.04 M) at 40 °C for 20 h. <sup>b</sup>Determined by chiral HPLC. <sup>c</sup>The Rh-H<sub>2</sub>L and Rh-Me<sub>2</sub>L complexes are insoluble in the reaction solvents. <sup>d</sup>Yield determined by NMR integration.

**Table 2. Asymmetric AlMe<sub>3</sub> Additions to  $\alpha,\beta$ -Unsaturated Ketones Catalyzed by 1·Rh and Homogenous Control Catalyst**

entry	substrate	catalyst	conv.%	e.e.% <sup>a</sup>	Isolated yield <sup>b</sup>
1		1·Rh	97	98	71%
2		Rh-Me <sub>2</sub> L	82	>99	46%
3		1·Rh	97	99	68%
4		Rh-Me <sub>2</sub> L	91	>99	<40%

<sup>a</sup>Determined by GC. <sup>b</sup>Isolated yields are much lower due to the relatively low boiling points of the allylic alcohols **6**.

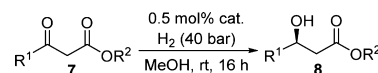
cyclohexenone (Table 1).<sup>16</sup> At 1 mol% catalyst loadings, 1·Rh afforded conjugate addition products **4** in nearly quantitative conversions with 80–99% isolated yields (entries 1–3, Table 1). Under the same conditions, neither the Rh-Me<sub>2</sub>L nor Rh-H<sub>2</sub>L control gave appreciable amounts of products due to their insolubility in the reaction solvents, whereas the Rh-BINAP homogeneous control gave modest isolated yields of 29–46% (entries 6–8, Table 1). In fact, 3 mol% of the Rh-BINAP catalyst was needed to afford the addition products in yields comparable (entries 9–11, Table 1) to those produced by 1 mol% of 1·Rh. The ee's of the conjugate addition products (99% or higher) are similar between 1·Rh and the homogeneous control, but the activity of 1·Rh is ~3 times as high as that of the homogeneous control. We believe that site isolation of the active catalysts in 1·Rh is responsible for its higher catalytic activity, by preventing any intermolecular catalyst deactivation pathways.

1·Rh also showed excellent activity in additions of AlMe<sub>3</sub> to  $\alpha,\beta$ -unsaturated ketones to afford chiral allylic alcohols **6** (Table 2).<sup>17</sup> At 0.4 mol% catalyst loadings, 1·Rh afforded allylic alcohols in nearly quantitative conversions and 71% and 68% isolated

yields for **6a** and **6b**, respectively. At the same catalyst loadings, the conversions and yields observed for 1·Rh are higher than those for the Rh-Me<sub>2</sub>L homogeneous control. The ee's seen for 1·Rh are comparable to those for the Rh-Me<sub>2</sub>L homogeneous control. 1·Rh is thus an excellent single-site solid asymmetric catalyst for multiple organic addition reactions.

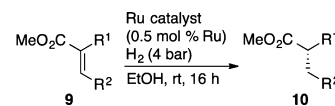
We have carried out a number of experiments to demonstrate the “heterogeneous” nature of 1·Rh. First, the PXRD of 1·Rh recovered from the reaction between AlMe<sub>3</sub> and 2-cyclohexenone (**2a**) remained the same as those of freshly prepared **1** and 1·Rh (Figure 2c). Second, at a 0.4 mol% catalyst loading, the 1·Rh catalyst could be recovered and reused for AlMe<sub>3</sub> addition to **2a** with only slight decreases in conversions and enantioselectivities. The conversions/ee's for three consecutive runs (with recovered 1·Rh) are 96/99%, 95/98%, and 87/96%, respectively. Third, the amount of Rh and Zr leaching into the supernatant during the AlMe<sub>3</sub> addition reaction to **2a** is <0.4% and 1.0%, as determined by ICP-MS. Further, the amount of Rh and Zr leaching into the supernatant during phenylboronic acid addition to **2a** is <0.9% and 0.2%, as determined by ICP-MS. Finally, the 1·Rh recovered from the reaction between **2a** and *m*-methylcarboxyphenylboronic acid (85% isolated yield, 99% ee) could be reused to catalyze addition of *p*-acetylphenylboronic acid (65% isolated yield, 99% ee), whereas removal of 1·Rh 1 h after the reaction between **2a** and *m*-methylcarboxyphenylboronic acid completely stopped the reaction (Scheme S1). All of the above evidence strongly supports the notion that 1·Rh is a recoverable and reusable, highly active, enantioselective single-site solid catalyst.

1·Ru is highly active in hydrogenation of  $\beta$ -keto esters (Table 3)<sup>8b,18</sup> and substituted alkenes (Table 4).<sup>19</sup> Under H<sub>2</sub> at 40 bar,

**Table 3. Asymmetric Hydrogenation of  $\beta$ -Keto Esters by 1·Ru and Ru(Me<sub>2</sub>L)(DMF)<sub>2</sub>Cl<sub>2</sub>**

entry	R <sup>1</sup>	R <sup>2</sup>	catalyst	yield <sup>a</sup>	ee (%) <sup>a</sup>
1	Me	Me	1·Ru	quant.	97
2	Et	Et	1·Ru	quant.	94
3	Me	<sup>t</sup> Bu	1·Ru	quant.	96
4	Me	Me	Ru(Me <sub>2</sub> L)(DMF) <sub>2</sub> Cl <sub>2</sub>	quant.	>99
5	Et	Et	Ru(Me <sub>2</sub> L)(DMF) <sub>2</sub> Cl <sub>2</sub>	quant.	>99
6	Me	<sup>t</sup> Bu	Ru(Me <sub>2</sub> L)(DMF) <sub>2</sub> Cl <sub>2</sub>	quant.	>99

<sup>a</sup>Determined by GC.

**Table 4. Asymmetric Hydrogenation of Substituted Alkenes by 1·Ru and Ru(Me<sub>2</sub>L)(DMF)<sub>2</sub>Cl<sub>2</sub>**

entry	R <sup>1</sup>	R <sup>2</sup>	catalyst	yield <sup>a</sup>	ee (%) <sup>a</sup>
1	NHAc	H	1·Ru	quant.	85
2 <sup>b</sup>	NHAc	Ph	1·Ru	quant.	70
3	CH <sub>2</sub> CO <sub>2</sub> Me	H	1·Ru	quant.	91
4	NHAc	H	Ru(Me <sub>2</sub> L)(DMF) <sub>2</sub> Cl <sub>2</sub>	quant.	88
5	NHAc	Ph	Ru(Me <sub>2</sub> L)(DMF) <sub>2</sub> Cl <sub>2</sub>	quant.	81
6	CH <sub>2</sub> CO <sub>2</sub> Me	H	Ru(Me <sub>2</sub> L)(DMF) <sub>2</sub> Cl <sub>2</sub>	quant.	96

<sup>a</sup>Determined by GC. <sup>b</sup>H<sub>2</sub> (40 bar).

1-Ru converted methyl acetoacetate to the corresponding alcohol in a quantitative yield with ee's as high as 97%. By varying the post-synthetic metalation conditions, ee's as high as 98% could be obtained for hydrogenation of *tert*-butyl acetoacetate, albeit in lower yields (51%, SI). 1-Ru is active in hydrogenating a broad range of  $\beta$ -keto esters, but the ee's of the hydrogenation products are 2–5% lower than those obtained using Ru(Me<sub>2</sub>L)(DMF)<sub>2</sub>Cl<sub>2</sub>.

1-Ru also catalyzed hydrogenation of substituted alkenes at low pressures and room temperature (Table 4). First, 0.5 mol% of 1-Ru catalyzed hydrogenation of 9a–9c to afford 10a–10c in quantitative yields and 70–91% ee's. As with hydrogenation of  $\beta$ -keto esters, the ee's of 10a–10c are 3–11% lower for the 1-Ru-catalyzed reactions than for those catalyzed by Ru(Me<sub>2</sub>L)(DMF)<sub>2</sub>Cl<sub>2</sub>. We believe that the metalation procedure has not yet been optimized for 1-Ru and a small amount of achiral Ru complex might have been trapped in the MOF channel, contributing to the racemic background reaction. Inductively coupled plasma-optical emission spectroscopy showed the leaching of 3.6% Ru but only 0.1% Zr from the substituted alkene (methyl 2-acetamidoacrylate) hydrogenation reaction. The much lower Zr concentration in the supernatant indicates that the Ru present in solution is more likely the result of either trapped achiral Ru complexes, such as Ru(cod)(2-methylallyl)<sub>2</sub>, or the Ru species dissociating from the L ligand, but not from dissolution of the MOF. This small amount of achiral Ru complex would have been below the sensitivity of the XAFS technique. Several tests also demonstrated the "heterogeneous" nature and the ability to reuse 1-Ru in asymmetric hydrogenation reactions (Scheme S3 and Figures S57–S58).

In summary, we report the first example of a BINAP-based MOF and its post-synthetic metalation to afford highly active and enantioselective catalysts. The 1-Rh catalyst is 3 times as active as the homogeneous control and produces aryl addition products at ee's of >99%. XAFS studies demonstrated that 1-Ru has the same Ru coordination environment as the homogeneous control. The post-synthetically metalated BINAP-MOFs thus provide a versatile family of single-site solid catalysts for a broad scope of asymmetric organic transformations, and can potentially find application in practical synthesis of fine chemicals.

## ■ ASSOCIATED CONTENT

### Supporting Information

Experimental details and characterization data. This material is available free of charge via the Internet at <http://pubs.acs.org>.

## ■ AUTHOR INFORMATION

### Corresponding Author

wenbinlin@uchicago.edu

### Author Contributions

†J.M.F. and T.S. contributed equally.

### Notes

The authors declare no competing financial interest.

## ■ ACKNOWLEDGMENTS

W.L. thanks NSF (CHE-1111490) for financial support. J.M.F. was supported by a U.S. DOE Office of Science Graduate Fellowship (DE-AC05-06OR23100). J.V.L. acknowledges the ACS Petroleum Research Fund for financial support (grant no. 52148-DN15). Use of the National Synchrotron Light Source, Brookhaven National Laboratory, was supported by the U.S. DOE Office of Science (contract no. DE-AC02-98CH10886).

## ■ REFERENCES

- (1) (a) Moulton, B.; Zaworotko, M. J. *Chem. Rev.* **2001**, *101*, 1629. (b) Evans, O. R.; Lin, W. *Acc. Chem. Res.* **2002**, *35*, 511. (c) Lan, A.; Li, K.; Wu, H.; Olson, D. H.; Emge, T. J.; Ki, W.; Hong, M.; Li, J. *Angew. Chem., Int. Ed.* **2009**, *48*, 2334. (d) Uemura, T.; Yanai, N.; Kitagawa, S. *Chem. Soc. Rev.* **2009**, *38*, 1228. (e) Das, M. C.; Xiang, S.; Zhang, Z.; Chen, B. *Angew. Chem., Int. Ed.* **2011**, *50*, 10510. (f) Wiers, B. M.; Foo, M.-L.; Balsara, N. P.; Long, J. R. *J. Am. Chem. Soc.* **2011**, *133*, 14522. (g) Kreno, L. E.; Leong, K.; Farha, O. K.; Allendorf, M.; Van Duyne, R. P.; Hupp, J. T. *Chem. Rev.* **2012**, *112*, 1105. (h) Li, J.-R.; Sculley, J.; Zhou, H.-C. *Chem. Rev.* **2012**, *112*, 869. (i) Furukawa, H.; Cordova, K. E.; O'Keeffe, M.; Yaghi, O. M. *Science* **2013**, *341*. (j) Shustova, N. B.; Cozzolino, A. F.; Reineke, S.; Baldo, M.; Dincă, M. *J. Am. Chem. Soc.* **2013**, *135*, 13326.
- (2) Kesanli, B.; Lin, W. *Coord. Chem. Rev.* **2003**, *246*, 305.
- (3) (a) Yoon, T. P.; Jacobsen, E. N. *Science* **2003**, *299*, 1691. (b) Ma, L.; Abney, C.; Lin, W. *Chem. Soc. Rev.* **2009**, *38*, 1248. (c) Falkowski, J. M.; Liu, S.; Lin, W. *Isr. J. Chem.* **2012**, *52*, 591. (d) Yoon, M.; Srirambalaji, R.; Kim, K. *Chem. Rev.* **2012**, *112*, 1196.
- (4) (a) Evans, O. R.; Ngo, H. L.; Lin, W. *J. Am. Chem. Soc.* **2001**, *123*, 10395. (b) Wu, C. D.; Hu, A.; Zhang, L.; Lin, W. *J. Am. Chem. Soc.* **2005**, *127*, 8940.
- (5) Cho, S.-H.; Ma, B.; Nguyen, S. T.; Hupp, J. T.; Albrecht-Schmitt, T. E. *Chem. Commun.* **2006**, 2563.
- (6) (a) Tanaka, K.; Oda, S.; Shiro, M. *Chem. Commun.* **2008**, 820. (b) Ma, L.; Falkowski, J. M.; Abney, C.; Lin, W. *Nat. Chem.* **2010**, *2*, 838. (c) Song, F.; Want, C.; Falkowski, J. M.; Ma, L.; Lin, W. *J. Am. Chem. Soc.* **2010**, *132*, 15390. (d) Falkowski, J. M.; Wang, C.; Liu, S.; Lin, W. *Angew. Chem., Int. Ed.* **2011**, *50*, 8674. (e) Zheng, M.; Liu, Y.; Wang, C.; Liu, S.; Lin, W. *Chem. Sci.* **2012**, *3*, 2623. (f) Zhu, C.; Yuan, G.; Chen, X.; Yang, Z.; Cui, Y. *J. Am. Chem. Soc.* **2012**, *134*, 8058.
- (7) (a) Zhou, Q.-L., Ed. *Privileged Chiral Ligands and Catalysts*; Wiley-VCH: Weinheim, 2011. (b) Hayashi, T.; Tomioka, K.; Yonemitsu, O. *Asymmetric Synthesis: Graphical Abstracts and Experimental Methods*; Gordon and Breach: Tokyo, 1998.
- (8) (a) Miyashita, A.; Yasuda, A.; Takaya, H.; Toriumi, K.; Ito, T.; Souchi, T.; Noyori, R. *J. Am. Chem. Soc.* **1980**, *102*, 7932. (b) Noyori, R.; Takaya, H. *Acc. Chem. Res.* **1990**, *23*, 345.
- (9) (a) Hu, A.; Ngo, H. L.; Lin, W. *Angew. Chem., Int. Ed.* **2003**, *42*, 6000. (b) Hu, A.; Ngo, H. L.; Lin, W. *J. Am. Chem. Soc.* **2003**, *125*, 11490.
- (10) (a) Cavka, J. H.; Jakobsen, S.; Olsbye, U.; Guillou, N.; Lamberti, C.; Bordiga, S.; Lillerud, K. P. *J. Am. Chem. Soc.* **2008**, *130*, 13850. (b) Kandiah, M.; Nilsen, M. H.; Usseglio, S.; Jakobsen, S.; Olsbye, U.; Tilsted, M.; Larabi, C.; Quadrelli, E. A.; Bonino, F.; Lillerud, K. P. *Chem. Mater.* **2010**, *22*, 6632.
- (11) Hu, A.; Ngo, H. L.; Lin, W. *Angew. Chem., Int. Ed.* **2004**, *43*, 2501.
- (12) From the commercially available starting material BINAP, the overall yield for H<sub>2</sub>L is 9.0% in eight steps.
- (13) Férey, G.; Mellot-Draznieks, C.; Serre, C.; Millange, F. *Acc. Chem. Res.* **2005**, *38*, 217.
- (14) Cohen, S. M. *Chem. Rev.* **2012**, *112*, 970.
- (15) Attempts to measure Rh K-edge spectra of the analogous Rh complex and 1-Rh were unsuccessful due to absorption signal interference from Rh-coated X-ray mirrors used at Beamline X18A at NSLS.
- (16) (a) Takaya, Y.; Ogasawara, M.; Hayashi, T.; Sakai, M.; Miyaura, N. *J. Am. Chem. Soc.* **1998**, *120*, 5579. (b) Hayashi, T.; Yamasaki, K. *Chem. Rev.* **2003**, *103*, 2829.
- (17) Siewert, J.; Sandmann, R.; von Zezschwitz, P. *Angew. Chem., Int. Ed.* **2007**, *46*, 7122.
- (18) (a) Noyori, R.; Ohkuma, T.; Kitamura, M.; Takaya, H.; Sayo, N.; Kumobayashi, H.; Akutagawa, S. *J. Am. Chem. Soc.* **1987**, *109*, 5856. (b) Noyori, R. *Angew. Chem., Int. Ed.* **2002**, *41*, 2008.
- (19) Ohta, T.; Takaya, H.; Kitamura, M.; Nagai, K.; Noyori, R. *J. Org. Chem.* **1987**, *52*, 3174.